Nuclear Engineering and Technology 56 (2024) 601–610

Contents lists available at ScienceDirect

Nuclear Engineering and Technology

journal homepage: www.elsevier.com/locate/net

Original Article

An extensive characterization of xenon isotopic activity ratios from nuclear explosion and nuclear reactors in neighboring countries of South Korea

Ser Gi Hong *, Geon Hee Park, Sang Woo Kim, Yu Yeon Cho

Department of Nuclear Engineering, Hanyang University, 222 Wangsimni-ro, Seongdong-gu, Seoul, 04763, South Korea

ARTICLE INFO

Keywords:
Xenon isotopic ratio
Nuclear test
5MWe Yongbyon reactor
Source discrimination

ABSTRACT

This paper gives an extensive analysis on the characterization of xenon isotopic ratios for various nuclear reactors and nuclear explosions through neutronic depletion codes. The results of the characterization can be used for discriminating the sources of the xenon isotopes' release among the nuclear explosions and nuclear reactors. The considered sources of the xenon radionuclides do not only include PWR, CANDU, and nuclear explosions using uranium and plutonium bombs, but also IRT-200 and 5MWe Yongbyon (MAGNOX reactor) research reactors operated in North Korea. A new data base (DB) on xenon isotopic activity ratios was produced using the results of the characterization, which can be used in discrimination of the sources of xenon isotopes. The results of the study show that 5MWe Yongbyon reactor has quite different characteristics in $^{135}Xe/^{133}Xe$ ratio from the PWRs and the nuclear reactors have different characteristics in $^{135}Xe/^{133}Xe$ ratios from the nuclear explosions.

1. Introduction

North Korea has conducted six nuclear tests since 2006, which were serious threat for the world including South Korea. Recently, there have been some signs on repairing the underground tunnels at the Pung-gye-ri nuclear test site and on the re-operation of 5MWe Yongbyon reactor. So, the identification of the nuclear test based on some measured information is quite important. Internationally, CTBTO (Comprehensive Nuclear-Test-Ban Treaty Organization) uses four different types of monitoring techniques for nuclear tests. The radioactive gases and particulate nuclides are collected in the atmosphere from the control stations deployed through the International Monitoring System (IMS) established by CTBTO [1,2]. Of them, the radionuclide technology involved with the detection of radioactive noble gases and particles is the only one which can confirm whether an explosion is indicative of a nuclear test or not. Therefore, preparation of the reliable data on the release of atmospheric radioactivity from underground nuclear test explosions by the neighboring countries is important in developing and verifying methods of the nuclear test. Among the radioactive nuclides generated from nuclear explosions and nuclear facilities, four radioactive xenon isotopes ^{131m}Xe, ^{133m}Xe, ^{133}Xe, and ^{135}Xe monitored by IMS are considered as the relevant nuclides to identify the source of their releases because a substantial amount of these nuclides is released from nuclear explosion or civilian nuclear facilities and they have long half-lives (11.94, 2.19, 5.24 days, and 9.14 h, respectively) enough to be detected [2,3]. In particular, these nuclides are known as the only probable ones which can leak out even from the well-confined underground nuclear test relatively to many other non-gaseous fission product nuclides [3–5].

There have been several previous works on the characterization of isotopic ratios of the atmospheric xenon from PWRs and nuclear explosions because it is known that the isotopic activity ratios of ^{131m}Xe, ^{133m}Xe, ^{133}Xe, and ^{135}Xe isotopes are feasible to be used as the indicators of nuclear test [1–3]. Also, many other works have studied the identification of the location and time of the nuclear tests or reactor types including fuel burnups releasing these xenon isotopes based on measurements of the radioactive xenon isotopes [6–9].

However, to our knowledge, there have been no studies on characterization of the xenon isotopic ratios for the various reactors including 5MWe Yongbyon reactor, IRT-2000 reactors, PWRs and CANDUs for discriminating the xenon releases from these reactors and nuclear test. The objective of this work is to extensively characterize the xenon isotopic ratios using nuclear fuel depletion codes for the potential sources of the xenon isotopes' release from the neighboring countries of South Korea, and to prepare an extensive database which can be utilized for the identification of nuclear test.

Section 2 describes analysis method and models, and Section 3 gives the results and analysis of the modeling and simulations. Finally, the

* Corresponding author.
E-mail address: hongsergi@hanyang.ac.kr (S.G. Hong).

https://doi.org/10.1016/j.net.2023.10.037
Received 23 June 2023; Received in revised form 29 September 2023; Accepted 27 October 2023
Available online 27 October 2023

Table 1
Design specification of PWR assemblies.

Items	WH 17x17	CE 16x16
Fuel radius (cm)	0.3922	0.41275
Fuel clad thickness (cm)	0.05715	0.0635
Gap thickness (mm)	0.0785	0.0889
Guide tube or water hole Inner/outer radii (cm)	0.56135/0.602	1.143/1.2446
Pin pitch (cm)	1.2598	1.286
Fuel assembly pitch (cm)	21.4166	20.78

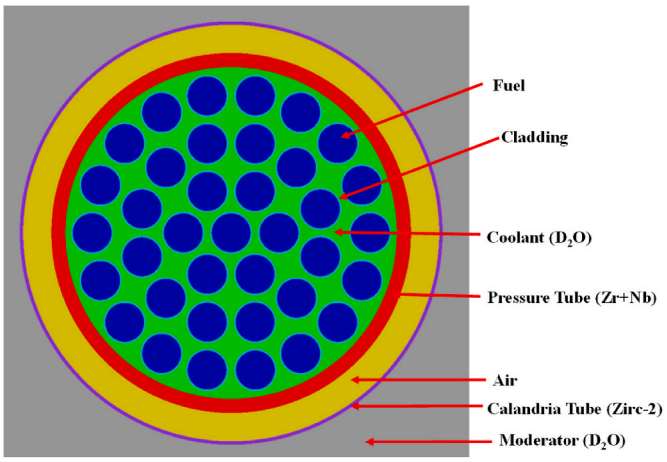

Fig. 1. Configurations of CANDU fuel bundle.

Table 2
Design specification of CANDU fuel bundle.

Item	Values
Fuel radius (cm)	0.6075
Cladding thickness (cm)	0.0465
Pressure tube inner radius (cm)	5.16
Pressure tube outer radius (cm)	5.60
Calandria tube inner radius (cm)	6.478
Calandria tube outer radius (cm)	6.587
Modeled region side length (cm)	28.575

summary and conclusions are presented in Section 4.

2. Analysis method and models

In this work, the xenon isotopic activity ratios from various nuclear reactors and nuclear bombs are evaluated by depletion calculations with ORIGEN [10] in SCALE6.2 [11] and Serpent [12] codes for various different conditions. The nuclear reactors which are considered as possibly being operated in the neighboring countries of South Korea are PWRs, CANDUs, 5MWe Yongbyon graphite moderated reactor, and IRT-2000. TRITON [11] was used for generating the burnup dependent effective one-group cross section libraries for the depletion analysis. ORIGEN in SCALE6.2 provides an advanced depletion solvers using CRAM (Chebyshev Rational Approximation) method for approximating the matrix exponential, which gives high accuracy. This CRAM option was adopted in this work. The NEWT option which employs the extended step characteristic method for transport calculation was used as the transport calculation option in TRITON. The effective one-group cross section libraries were prepared as function of burnup, uranium enrichment, moderator density, boron concentration, and fuel temperatures.

Usually, the reactor-specific effective one-group cross sections are generated using a single fuel assembly or other unit lattice structures

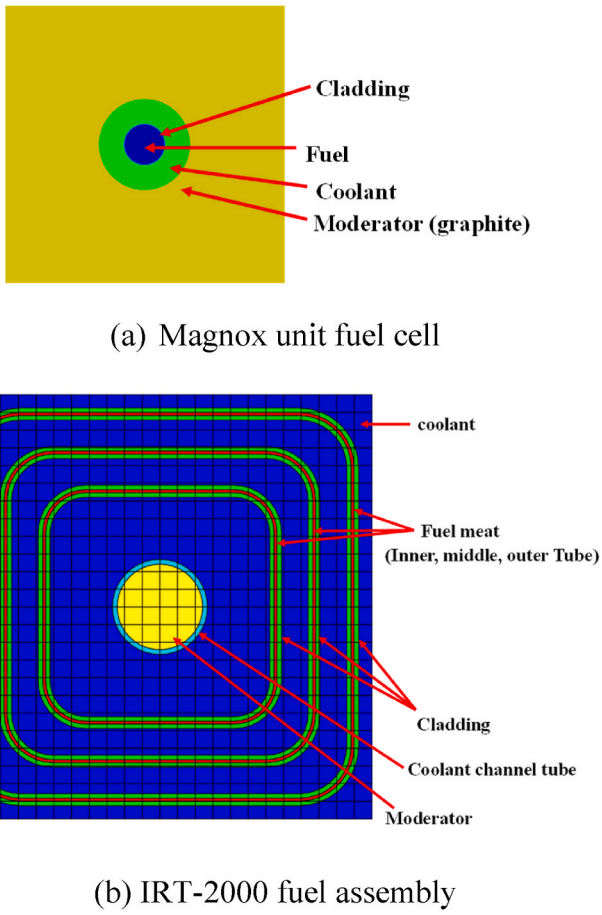

Fig. 2. Configurations of MAGNOX unit fuel cell and IRT-2000 fuel assembly.

Table 3
Design specification of IRT-2000 fuel assembly.

Item	Values
Uranium enrichment (%) of fuel	36.0
Specific power (W/g)	514.29
Fuel cladding thickness (cm)	0.075
Fuel thickness (cm)	0.05
Distance between fuel tubes (cm)	0.45
Inner radius of central hole (cm)	0.72
Thickness of central hole (cm)	0.08
Distance from innermost tube to the center of the central hole (cm)	1.85
Pitch of the assembly (cm)	7.15

rather than using whole core because the whole core depletion calculations require very high computing costs. For PWRs, we considered typical WH (WeshtingHouse) type 17x17 fuel assembly [13] and CE (Combustion Engineering) type 16x16 one [13]. Table 1 specifies the design parameters of these two fuel assemblies.

We considered various uranium enrichments of 1.5–5.0 wt% and various specific powers (20~60W/g) around a typical value of 40W/g to show their effects on the xenon isotopic activity ratios. We simulated three subsequent cycles of 375 EFPDs (Effective Full Power Day) with 60 days cooling for refueling between cycles.

For CANDU, a single fuel bundle comprised of 37 fuel rods of natural uranium oxide is considered as shown in Fig. 1. Table 2 summarizes the design data for the CANDU fuel bundle model [13]. As shown in Fig. 1, the fuel rods are located in a 4.443 mm pressure tube (Zr-2.5 wt%Nb), which is subsequently surrounded by a 8.746 mm thick gap region and a 1.097 mm thick calandria tube of Zircaloy-2. The outer region of the pressure tube was modeled with a large D_2O moderator region. Different

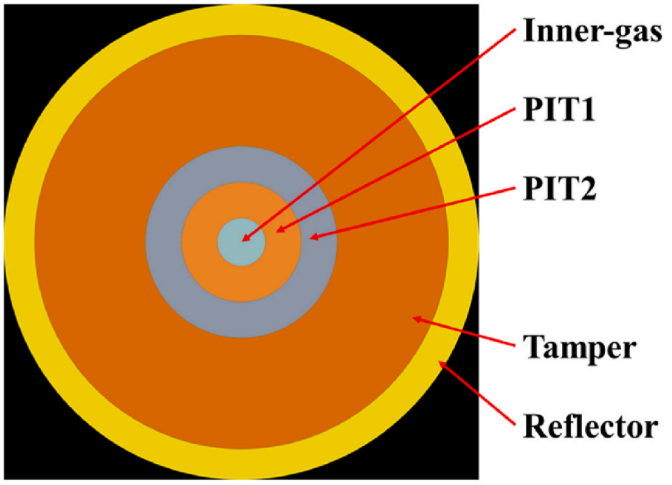

Fig. 3. (Modeling configuration of WG plutonium bomb).

Table 4
Modeling parameters of WG plutonium bomb.

Region	Composition	Density (g/cm^3)	Radius (cm)
Inner gas	^{3}H	0.251	2.0
PIT1	99 wt%WG Pu (93 wt%^{239}Pu/7 wt %^{240}Pu)+1 wt%Ga	15.589	5.0
PIT2	Uranium metal (90 wt% ^{235}U/10 wt% ^{238}U)	18.5	8.0
Tamper	^{238}U	19.1	17.25
Reflector	^{9}Be	1.848	19.82

specific powers of 15~25 W/g are considered with natural uranium oxide fuel to show their effects on the xenon isotopic activity ratios.

The 5MWe Youngbyon reactor which was used to generate weapon-grade (WG) plutonium in North Korea is the MAGONX type that uses CO_2 and graphite as the coolant and moderator, respectively [14]. In particular, this reactor uses the MAGNOX cladding (i.e., 0.8 % Al, 0.17 % Be, and 99 % Mg) and natural uranium metal fuel (U-0.5 % Al). In this work, we modeled a single square fuel channel in which the central fuel is sequentially surrounded by the clad and moderator. The fuel meat radius and clad thickness are 1.45 cm and 0.05 cm, respectively. The size of the single fuel channel is 20.0 cm. Fig. 2(a) shows the configuration of the single square fuel channel. For this reactor, the different specific powers ranging from 0.25 to 0.5W/g are considered to show the effect of the specific power on xenon isotopic activity ratios.

The IRT-2000 Reactor constructed in March 1963 in the Yongbyon nuclear research center is a pool type reactor which is cooled and moderated by light water. This reactor was subsequently upgraded three times from the initial 2 MW power using 10 % enriched uranium fuel to the 8 MW power with ~36.0 wt% enriched uranium one. For this reactor, a fuel lattice is comprised of three rectangular fuel plates of UO_2 and the water fills the coolant region between fuel plates. The cladding is 0.75 mm thick aluminum, which surrounds 0.5 mm thick fuel meat. The literatures give high specific power of 514.29 W/g and a fuel density of 2.63 g/cm^3 [13]. Table 3 summarizes the parameters of IRT-2000 fuel assembly. Fig. 2(b) shows the configuration of a fuel assembly of IRT-2000 used for depletion analysis. This model is adopted from the template of IRT-2000 given in SCALE6.2 [13].

A simple metal spherical model of 20 cm diameter without reflector was used for uranium bomb of 90 % enriched uranium metal, which corresponds to ~77.5 kg HEU (Highly Enriched Uranium) with 18.5 g/cm^3 density. The Serpent Monte Carlo calculation [12] for this condition

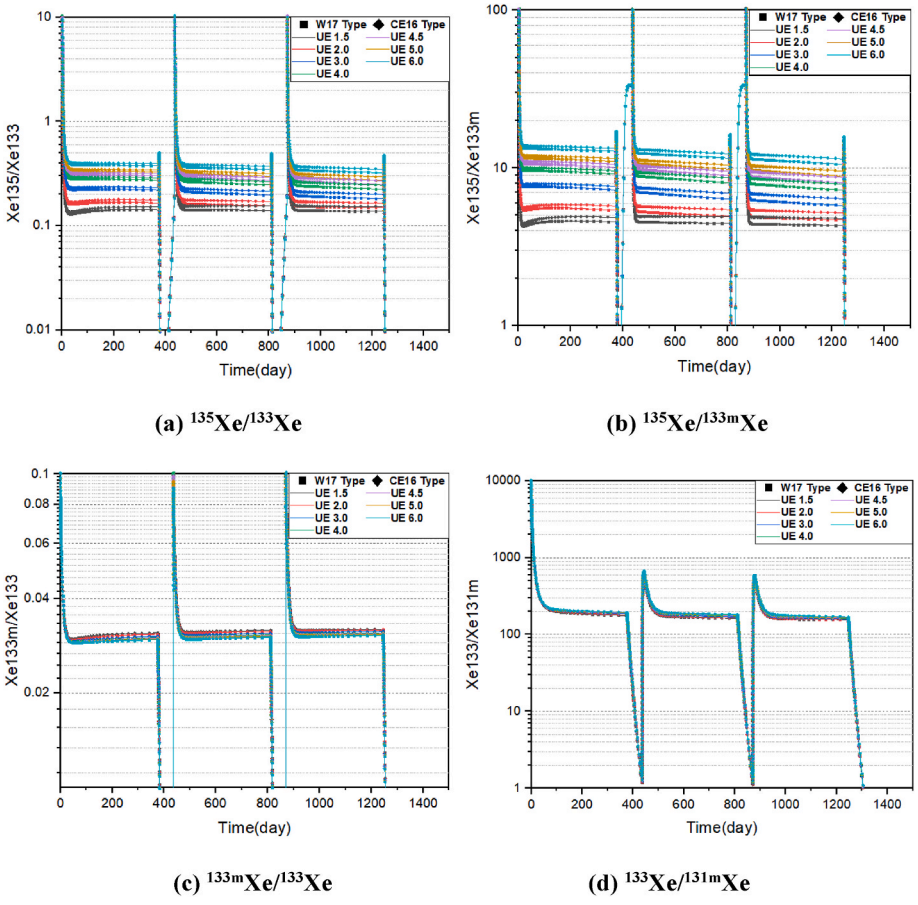

Fig. 4. Xe isotopic activity ratio as time for PWR for different uranium enrichments.

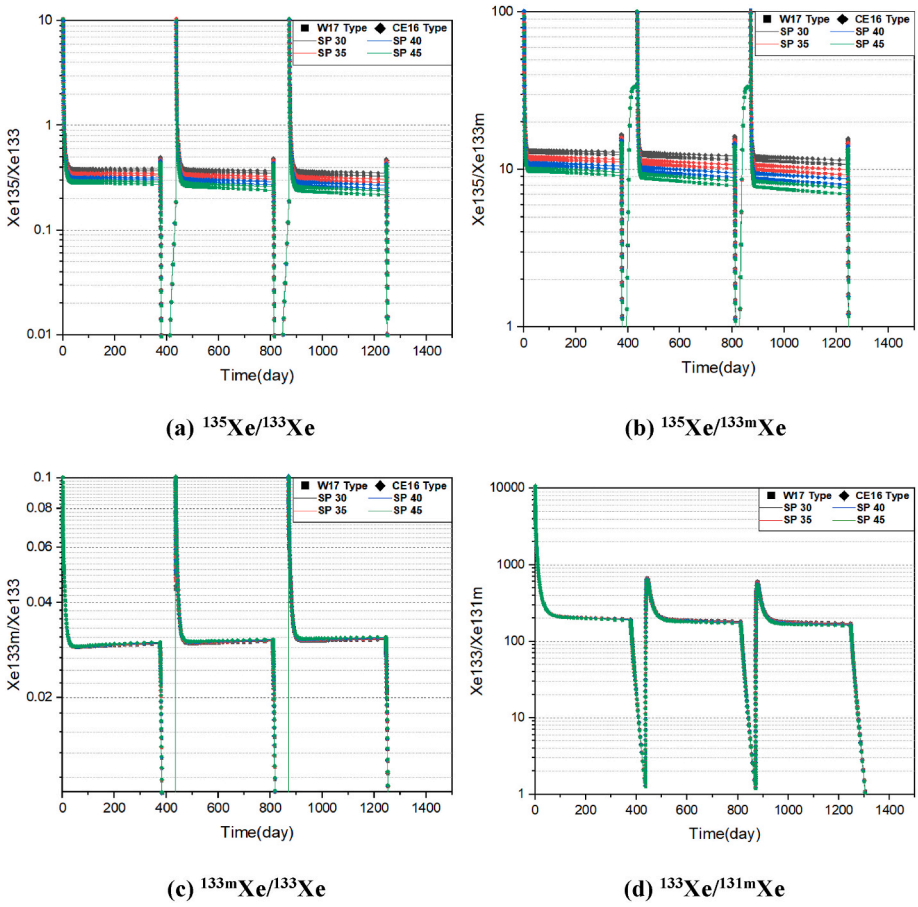

Fig. 5. Xe isotopic activity ratios as time for PWR for different specific power.

gives an effective multiplication factor of 1.0791. On the other hand, a slightly more detailed model shown in Fig. 3 was considered for WG (Weapon Grade) plutonium bomb. The WG plutonium metal (93 %^{239}Pu) mixed with 1 wt% Ga is loaded in the PIT1 region which is subsequently surrounded by HEU metal (PIT2), ^{238}U tamper, and ^{9}Be reflector [15]. For this configuration, the Serpent Monte Carlo calculation gives an effective multiplication factor of 1.30781. Table 4 summarizes the modeling parameters for the WG plutonium bomb.

3. Analysis and results

In this section, the results of the xenon isotopic activity ratios obtained from the depletion and radioactive decay calculations for the considered nuclear reactors and nuclear bombs are presented [16] and their characteristics are analyzed.

3.1. Xenon isotopic activity ratios as time for nuclear reactors

First, the effects of the uranium enrichment and specific power on the xenon isotopic activity ratios are analyzed for PWR. As described in Sec. 2, three subsequent cycles of 375 EFPDs (Effective Full Power Day) with refueling interval of 60 days between cycles are simulated using ORIGEN. Fig. 4 shows the changes of the Xe isotopic activity ratios for different uranium enrichments with a fixed specific power of 40 W/g both for CE and WH type assemblies. From the figure, it is shown that the ratios having Xe-135 in the numerator at the equilibrium states are low for low uranium enrichments, which can be understood from that Xe-135 inventory decreases due to higher neutron flux resulted from lower uranium enrichments. However, the ratios not related with Xe-135 do not change much as uranium enrichment. Also, it is observed that there are no considerable differences in Xe isotopic ratios between WH and CE type reactors. The rapid increase of the ratios after power drop is due to the fast decreases of the nuclides in denominators during the equilibrium state of the nuclides in numerators. For example, ^{135}Xe reaches its equilibrium at low power faster due to its shorter half life than ^{133}Xe and so the activity ratio of ^{135}Xe/^{133}Xe will rapidly increase after the equilibrium state of ^{135}Xe. In this interpretation, the fact that the nuclides in the numerators have shorter half life than the ones in the denominators for all the ratios should be noted.

Next, Fig. 5 compares the changes of the Xe isotopic activity ratios for different specific powers in PWRs with a fixed initial uranium enrichment of 4.5 %. The figure shows that the higher specific power leads to the lower Xe isotopic ratios having Xe-135 in the numerator, which resulted from the higher neutron flux. However, the specific power does not much affect the ratios not having Xe-135.

The effects of specific power on the xenon isotopic activity ratios for CANDU and MAGNOX reactors are also analyzed. Fig. 6 compares the ^{135}Xe/^{133}Xe activity ratios for CANDU and MAGNOX for different specific powers. Similarly to the PWR cases, a higher specific power leads to the lower values of the ratios having Xe-135 in the numerator. However,

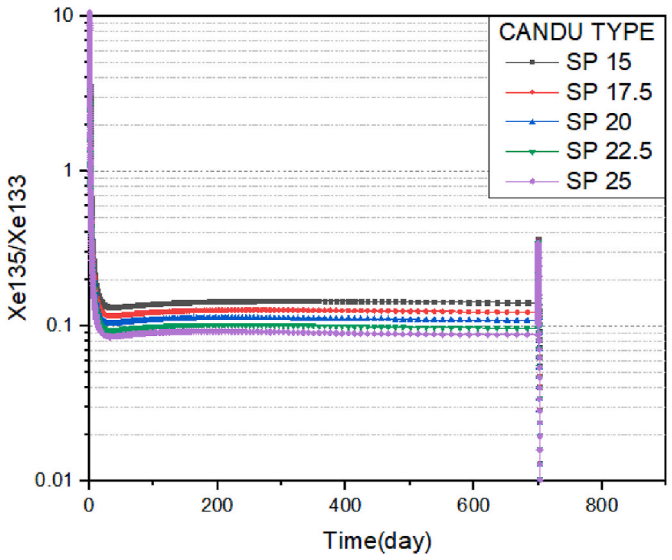

(a) CANDU

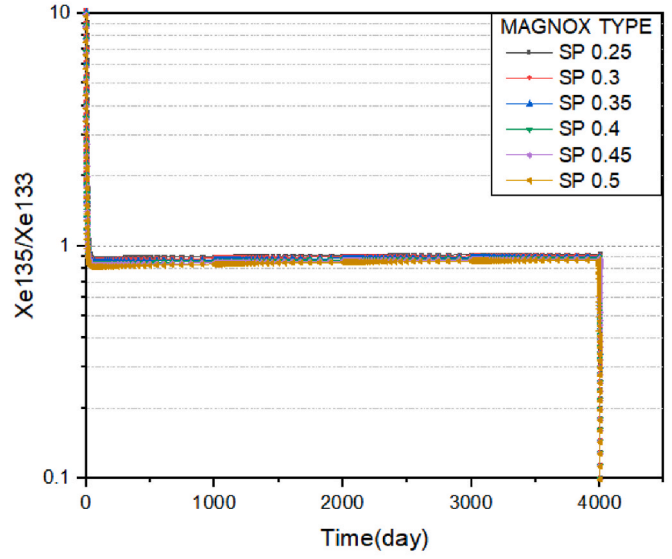

(b) MAGNOX

Fig. 6. $^{135}Xe/^{133}Xe$ activity ratios as time for CANDU and MAGNOX for different specific powers.

the considerable differences were not observed for different specific powers in MAGNOX due to its very low specific power.

Fig. 7 compares the changes of xenon isotopic activity ratios as time for all the considered reactors with their reference uranium enrichments and specific powers. The PWRs used 4.5 % uranium enrichment and 40W/g specific power as the reference values while CANDU, MAGNOX, and IRT-2000 used 20 W/g, 0.4 W/g, and 514.29 W/g, respectively, as the reference specific powers. For $^{135}Xe/^{133}Xe$ ratio, MAGNOX has the highest values and PWRs have the next highest values at the equilibrium states, while CANDU has lower values than them. For IRT-2000, it is noted that there is no equilibrium state over the considered operation time due to its very high specific power and the ratio is in similar level to CANDU. The other two ratios having Xe-135 in the numerator (i.e., $^{135}Xe/^{133m}Xe$ and $^{135}Xe/^{131m}Xe$ ratios) have the similar trend to that shown in $^{135}Xe/^{133}Xe$ ratio. The high values of these ratios for MAGNOX can be understood by the fact that it has very low specific power in spite of its low uranium enrichment because a low specific power leads to lower thermal flux level, while the low values for CANDU is due to the low uranium enrichment (i.e., natural uranium) and higher moderation resulted from a large amount of D_2O moderator, leading to high thermal flux. For the ratios having no Xe-135, the different reactor types have different values of these ratios in equilibrium states but their discriminations are not much clear in log-scale as in the ratios having Xe-135. However, it can be observed that Fig. 6(e) and (f) show small differences in $^{133}Xe/^{131m}Xe$ and $^{133m}Xe/^{131m}Xe$ ratios among the different reactor types. In particular, MAGNOX shows higher values in these ratios.

3.2. Xenon isotopic activity ratios as time for nuclear bombs

As described in Sec. 2, the depletion calculation for HEU and WG plutonium bombs were performed using the Serpent 2 code with the point-wise cross sections generated based on ENDF/B-VII.r1. For HEU bomb, the depletion calculation was performed with the burnup which was calculated by

$$Burnup[MWd/kg] = \frac{Yield[kt] \times 4.184 \times 10^6[MJ/kt]}{8,640MJ/MWd \times UM[kg]}, \quad (1)$$

where *UM* represents the initial uranium mass. As described in Sec. 2, the initial uranium mass was assumed to be 77.5 kg. So, for example, 20 kt yield leads to 12.5 MWd/kg burnup. The burnup was divided into 40 burnup intervals in the depletion calculations. For WG plutonium bomb, the burnup was calculated with the same way, but the initial Pu mass was assumed to be 407 kg. Fig. 8(a) and (b) compare the changes of the Xe isotopic activity ratios as time for HEU and WG-Pu bombs, respectively. These results were obtained using 20 kt and 50 kt yields for HEU and WG-Plutonium bombs, respectively. In Fig. 8, the time scale of shake was used to represent the very short time interval over which the explosion occurs and 1 shake means 10^{-8} s. The explosion time interval was calculated based on the assumption that the energy of the yield from the explosion is generated during 56 shakes.

Fig. 8 shows that two bomb types have different values of Xenon isotopic activity ratios. In particular, the HEU bomb case shows higher values in $^{135}Xe/^{131m}Xe$, $^{133m}Xe/^{131m}Xe$, $^{133}Xe/^{131m}Xe$, and $^{133m}Xe/^{133}Xe$ ratios but lower values in $^{135}Xe/^{133m}Xe$ than the WG plutonium one. Also, the effect of the yields of the bomb was also analyzed but they did almost not affect the xenon isotopic activity ratios.

Next, we analyzed the Xenon isotopic activity ratios after the full energy generation. Over this time period, the inventories of the xenon isotopes change only due to the radioactive decays. However, the fractionation which explains the separation of the xenon isotopes from their parent nuclides should be considered in estimating the xenon isotopic activity ratios because the xenon isotopes can be generated from the radioactive decays of their parent nuclides before the complete fractionation. The fractionation represents the processes through which the radio-xenon nuclides are separated from their parent nuclides. The fractionation is specially important for underground nuclear test in which the fractionation of radionuclides can occur due to different characteristics in early-time cavity processes, transport through the

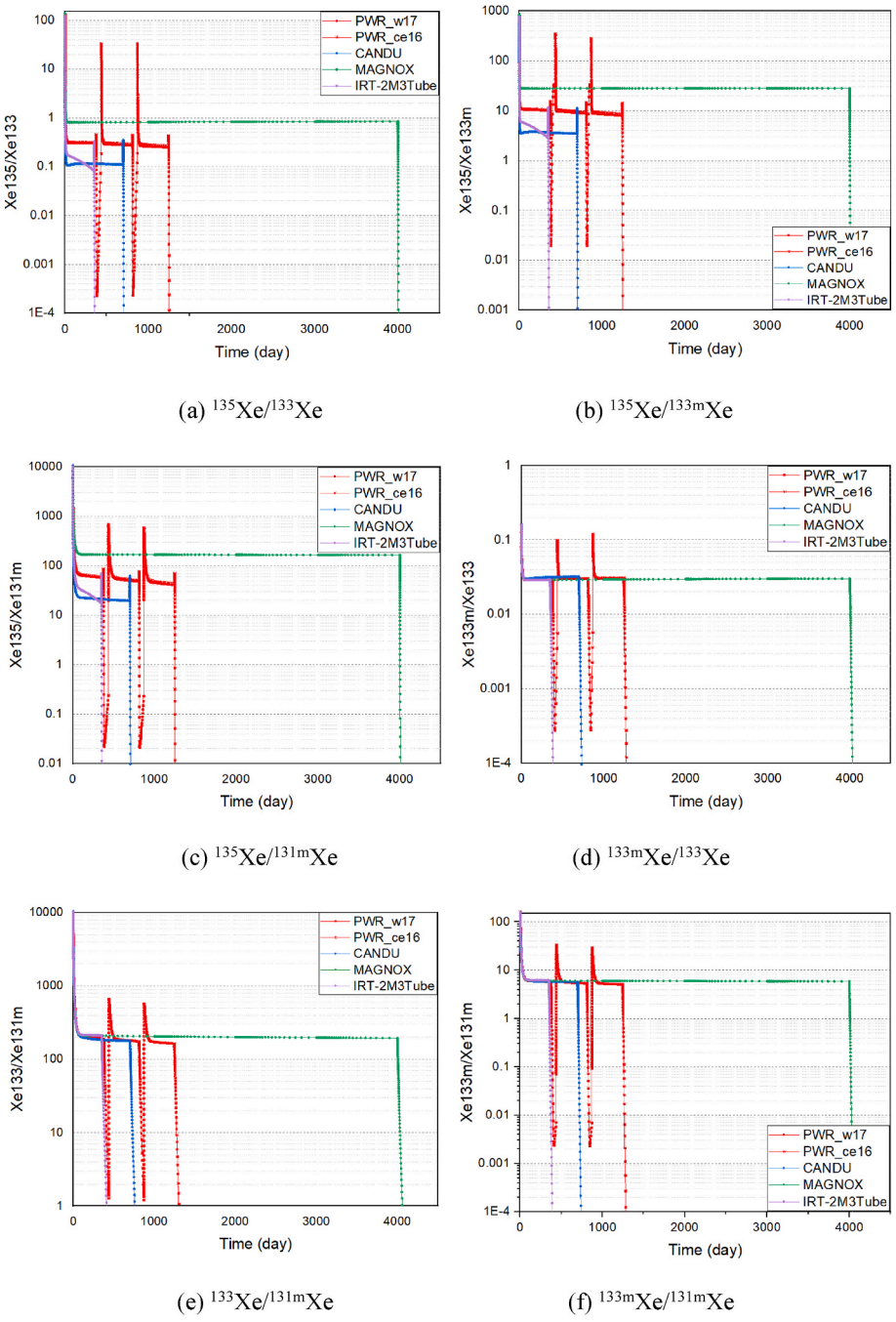

(a) $^{135}Xe/^{133}Xe$ (b) $^{135}Xe/^{133m}Xe$

(c) $^{135}Xe/^{131m}Xe$ (d) $^{133m}Xe/^{133}Xe$

(e) $^{133}Xe/^{131m}Xe$ (f) $^{133m}Xe/^{131m}Xe$

Fig. 7. Comparison of the Xe isotopic activity ratios for different reactor types.

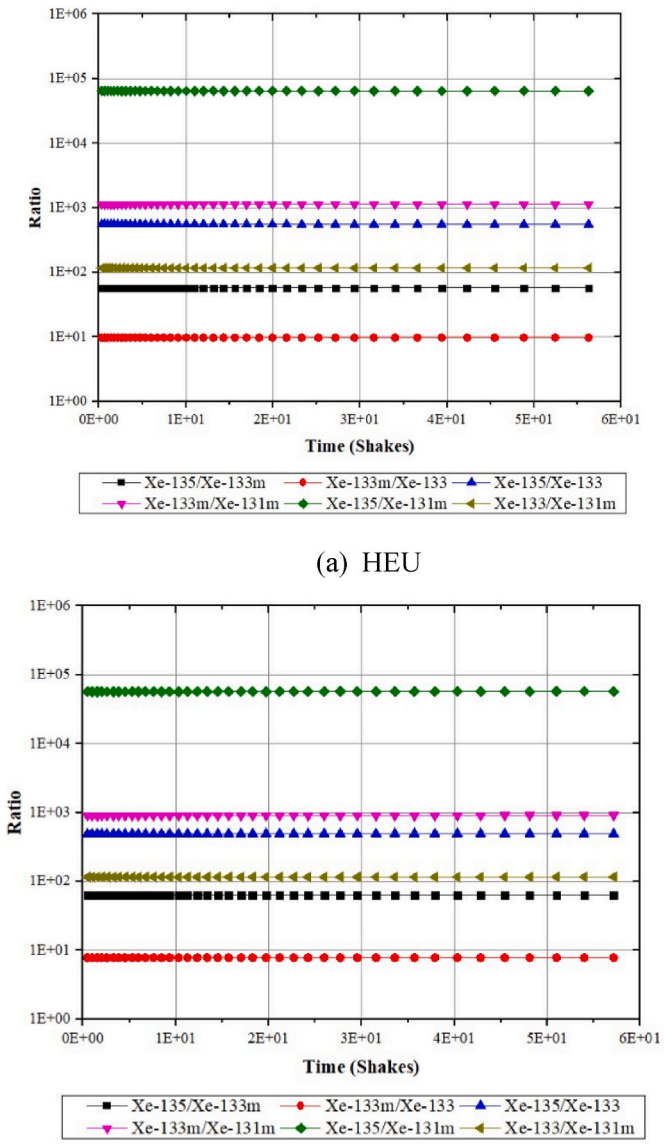

Fig. 8. Comparison of the Xe isotopic activity ratios for HEU and WG-Pu bombs.

rock, or dispersal through tunnels [17]. In this work, the effect of the fractionation time on the xenon isotopic activity ratio was analyzed for the time period after the full energy generation during explosion. Figs. 9–11 compare the changes of the $^{135}Xe/^{133}Xe$, $^{133m}Xe/^{133}Xe$, and $^{133}Xe/^{131m}$ activity ratios, respectively, for the HEU and WG Plutonium bombs after the full energy generation from explosion for different five fractionation times (i.e.,0.0, 0.01, 0.1, 1.0, and 10 h), and no fractionation case. The zero-fractionation time case means the prompt fractionation. After fractionation, it is important to note that the meta-stable xenon nuclides decay as time while their corresponding stable nuclides decay but also they can be produced from the decay of the meta-stable nuclides. These figures show that the fractionation significantly affects the isotopic activity ratios but there are no big differences in the trend of the isotopic activity ratios between HEU and WG Plutonium bombs in spites of their different levels.

From Figs. 9 and 11, it is shown that the activity ratios of $^{135}Xe/^{133}Xe$ and $^{133}Xe/^{131m}Xe$ increase when the fractionation occurs at the early times (i.e., 0.0, 0.01, and 0.1 h) and then decrease after their maximum values are reached. For example, the increase of $^{135}Xe/^{133}Xe$ can be understood by the contribution to ^{135}Xe from the rapid decay of ^{135m}Xe having 15.29 min half life but by slow decay of ^{133}Xe. Also, higher fission yield and branch ratio of ^{135m}Xe than those of ^{133m}Xe contributes to the increase of the $^{135}Xe/^{133}X$ activity ratio. From Figs. 9–11, it is also noted that the fractionation at later times slows down the decrease of the isotopic activity ratios, which can be also understood using the meta-stable nuclides.

Also, we analyzed the effects of the uranium enrichment and fissile content for HEU and WG Plutonium bombs, respectively, on the xenon isotopic activity ratios. They are included in the database which was utilized with machine learning techniques for the discrimination of the source of xenon release [18]. However, these results are not included in this paper due to their relatively small effects and to the limitation on the number of pages.

3.3. Relationship between xenon isotopic activity ratios

In this section, the relations between different xenon isotopic activity ratios are analyzed to show that they can give some insights for discriminations of the source of the release of xenon gases. The following six combinations of the xenon isotopic activity ratios are considered for all the considered reactors and nuclear bombs: 1) $^{135}Xe/^{133}Xe$ versus $^{133m}Xe/^{131m}Xe$, 2) $^{135}Xe/^{133}Xe$ versus $^{135}Xe/^{131m}Xe$, 3) $^{135}Xe/^{133m}Xe$ versus $^{135}Xe/^{133}Xe$, 4) $^{135}Xe/^{133m}Xe$ versus $^{135}Xe/^{131m}Xe$, 5) $^{133m}Xe/^{133}Xe$ versus $^{133m}Xe/^{131m}Xe$, and 6) $^{135}Xe/^{131m}Xe$ versus $^{133}Xe/^{131m}Xe$. The plots for these cases are given in Fig. 12(a)~(f). For the nuclear bombs, only fully fractionation and no fractionation cases

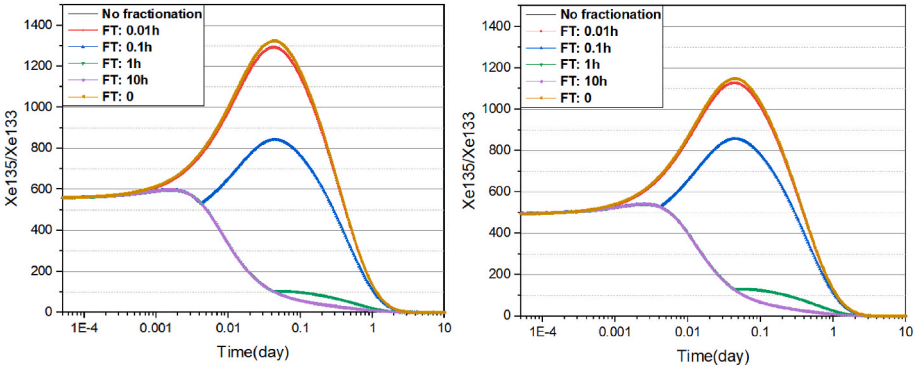

Fig. 9. Effects of the fractionation time (FT) on the $^{135}Xe/^{133}Xe$ activity ratio after full energy generation.

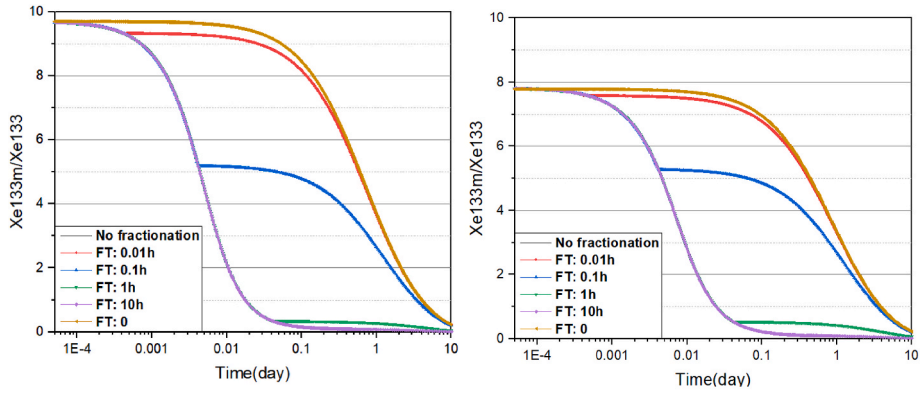

Fig. 10. Effects of the fractionation time (FT) on the $^{133m}Xe/^{133}Xe$ activity ratio after full energy generation.

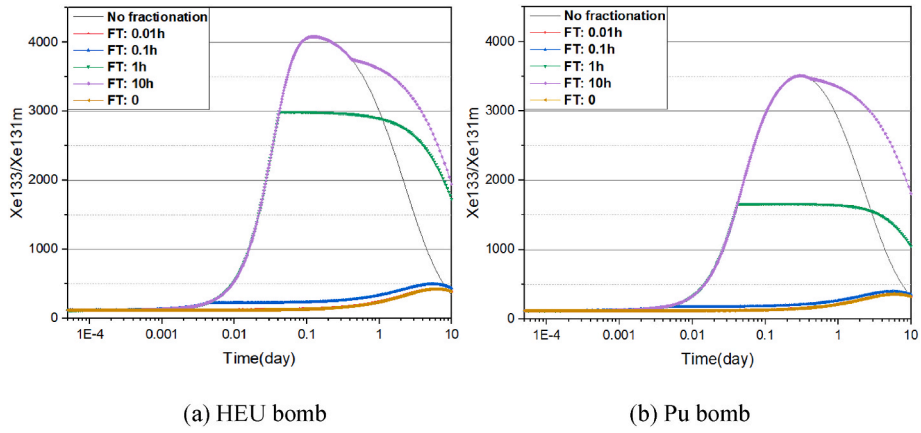

Fig. 11. Effects of the fractionation time (FT) on the $^{133}Xe/^{131m}Xe$ activity ratio after full energy generation.

are considered for simplicity. In the figures, the fully fractionation cases are denoted as "FT:0" while the other cases represent no fractionation cases. In these figures, the irradiations for all the reactors and bombs start at the right-upper part. The isotopic activity ratios reach their equilibrium states after their irradiation starts, and then they follow the change by radioactive decay. The closed curves for PWR are observed due to its cyclic operation. These figures show that they can be useful in discriminating the sources of xenon releases. For example, in Fig. 12(a), the reactors have different characteristics in the isotopic activity ratio changes from the nuclear bombs for the considered combinations of the isotopic activity ratios and the reactors also have their own characteristics from the others. The WG Plutonium and HEU bombs have very similar characteristics for the no fractionation cases relatively to the fully fractionation one. Also, it is shown from these figures that the different combinations of the isotopic activity ratios have different characteristics and so multiple use of these combinations will be helpful for the discrimination of xenon release sources.

4. Conclusions

In this paper, the xenon isotopic activity ratios were analyzed using simulations for various nuclear reactors, HEU and WG Pu bombs, to check if they can be useful for discrimination of xenon release sources. The considered nuclear reactors include PWRs, CANDU, IRT-2000, and 5MWe Yongbyon reactor (MAGNOX type). In particular, the last two reactors of them were considered because they were operated in North Korea. To cover the operational characteristics of the reactors, the variations of the specific power and uranium enrichment were considered. For HEU and WG Pu bombs, the effect of the fractionation time on the xenon isotopic activity ratios were analyzed. Additionally, the effects of bomb yield and uranium enrichment (or fissile content) were also analyzed and included in the database, but they were not included in this paper due to their relatively small effects and to the limitation on the number of pages.

The analysis showed that uranium enrichment and specific power significantly affect the xenon isotopic activity ratios (specially the ratios involved with ^{135}Xe) for nuclear reactors. Specifically, the ratios having ^{135}Xe in the numerator were low for low uranium enrichments and high specific powers at the equilibrium states. Among the considered reactors, for the ratios having ^{135}Xe in the numerator, MAGNOX has the highest values and PWRs have the next highest values at the equilibrium state, while CANDU has lower values than them. MAGNOX also showed higher values in $^{133}Xe/^{131m}Xe$ and $^{133m}Xe/^{131m}Xe$ ratios. Therefore, these characteristics of the xenon isotopic activity ratios are helpful for

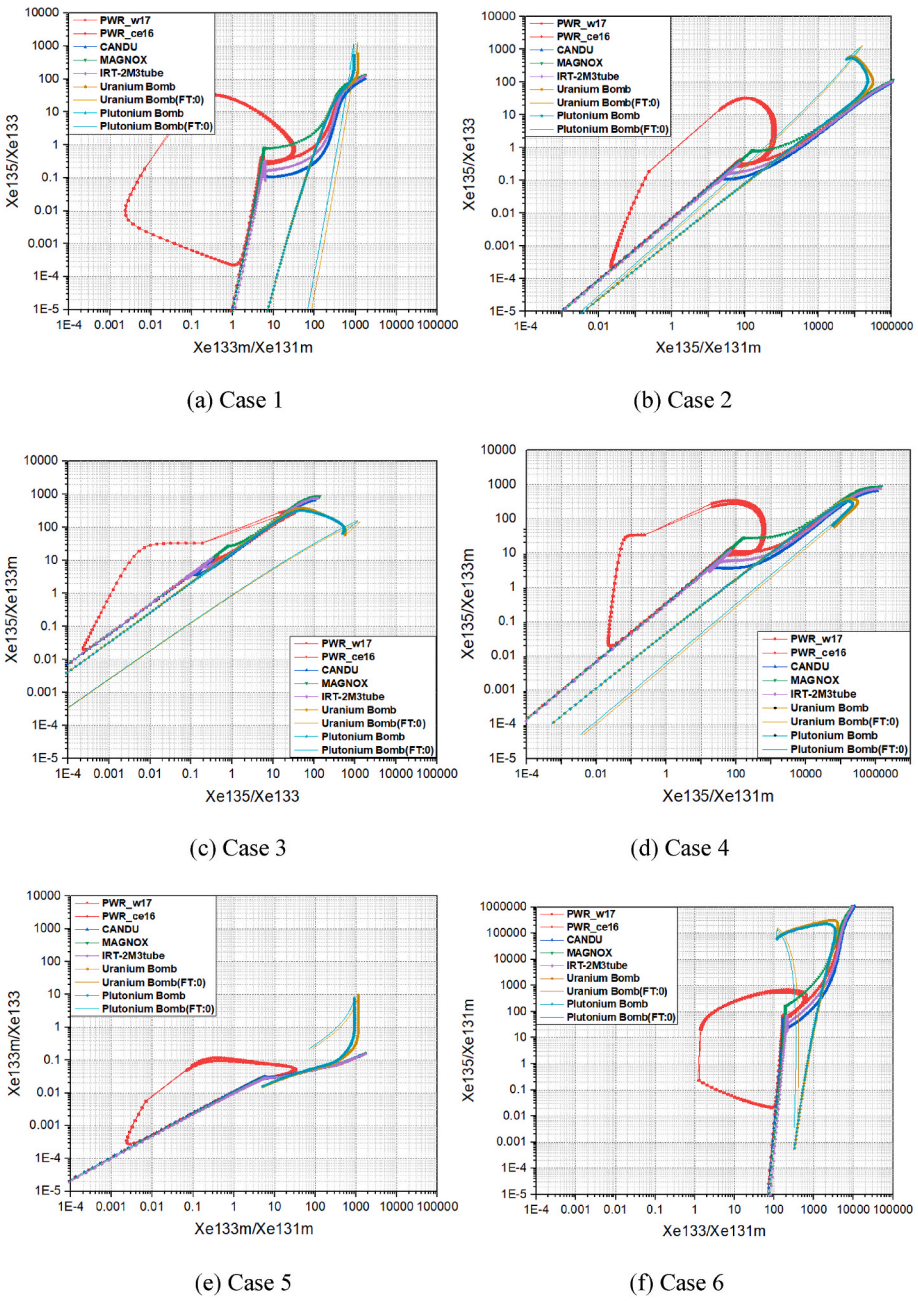

Fig. 12. Comparison of the relationships between different isotopic activity ratios.

discrimination among the reactors. CANDU also has distinct levels of the xenon isotopic activity ratios involving ^{135}Xe, which are also helpful for discriminations. For HEU and WG Pu bombs, the fractionation time significantly affects on the xenon isotopic ratios but the effects by fractionation time are similar between HEU and WG Pu bombs. Anyway, the effects of the fractionation time should be considered in the database for the discrimination. The analysis of the plots of the combinations of xenon isotopic activity ratios showed that the nuclear bombs have distinct characteristic curves from the nuclear reactors even with the consideration of the fractionation effects. Specifically, the lines of the nuclear bombs representing radioactive decays in the plots were well separated from those of the reactors, which helps the discrimination of the sources of xenon release. Also, it was found that the ratios involved with ^{135}Xe can be considered as good indicators in discriminating the xenon release sources and that with the combination of two xenon isotopic activity ratios, ^{135}Xe/^{133}Xe and ^{133m}Xe/^{131m}Xe seems to be a good indicator for the discrimination. However, multiple use of these combinations of xenon isotopic ratios would be helpful for better discrimination.

Declaration of competing interest

The authors declare that they have no known competing financial interests or personal relationships that could have appeared to influence the work reported in this paper.

Acknowledgments

This work was supported by the Nuclear Safety Research Program through the Korea Foundation Of Nuclear Safety (KoFONS) using the financial resource granted by the Nuclear Safety and Security Commission (NSSC) of the Republic of Korea. (No. 2103089).

References

[1] L.E. De Geer, "Radionuclide evidence for low-yield nuclear testing in North Korea in april/may 2010, Sci. Global Secur. 20 (2012) 1–29.

[2] M.B. Kalinowski, et al., Discrimination of nuclear explosions against civilian sources based on atmospheric xenon isotopic activity ratios, Pure Appl. Geophys. 167 (2010) 517–539.

[3] M.B. Kalinowski, Y.Y. Liao, "Isotopic characterization of radioiodine and radioxenon in releases from underground nuclear explosions with various degrees of fractionation, Pure Appl. Geophys. 171 (2014) 677–692.

[4] S.M. Bourret, E.M. Kwicklis, P.H. Stauffer, Evaluation of several relevant fractionation processes as possible explanation for radioxenon isotopic activity ratios in samples taken near underground nuclear explosions in shafts and tunnels, J. Environ. Radioact. 237 (2021), 106698.

[5] M.B. Kalinowski, Characterization of prompt and delayed atmospheric radioactivity releases from underground nuclear tests at Nevada as a function of release time, J. Environ. Radioact. 102 (2011) 824–836.

[6] A. Ringbom, et al., Radioxenon releases from A nuclear power plants : stack data and atmospheric measurements, Pure Appl. Geophys. 178 (2021) 2677–2693.

[7] A. Becker, G. Wotawa, A. Ringbom, P.R.J. Saey, Backtracking of noble gas measurements taken in the aftermath of the announced october 2006 event in North Korea by means of PTS methods in nuclear source estimation and reconstruction, Pure Appl. Geophys. 167 (2010) 581–599.

[8] M.B. Kalinowski, C. Pistner, " isotopic signature of atmospheric xenon released from light water reactors,", J. Environ. Radioact. 88 (2006) 215–235.

[9] P. D. Meutter, J. Camps, A. Delcloo, P. Termonia, "Assessment of the announced North Korean nuclear test using long-rang atmospheric transport and dispersion modeling," Sci. Rep., DOI:10.1038/s41598-017-07113-y..

[10] W.A. Wieselquist, The SCALE6.2 ORIGEN API for High Performance Depletion, ANS MC2015, Nashville, TN, 2015.

[11] B.T. Rearden, M.A. Jesse, SCALE Code System, ORNL/TM-2005/39, March 2018. Version 6.2.3.

[12] B. Ade, B. Betzler, ORIGEN Reactor Libraries, Oak Ridge National Laboratory, April 8, 2016.

[13] G.H. Park, S.G. Hong, An estimation of weapon-grade plutonium production from 5MWe yongbyun reactor through MCNP6 core depletion analysis, Prog. Nucl. Energy 130 (2020), 103533.

[14] J. Leppanen, M. Pusa, T. Viitanen, T. Kaltiaisenaho, "The serpent Monte Carlo code : status, development and application in 2013, Ann. Nucl. Energy 82 (2015) 142–150.

[15] R.K. Brown, Nuclear Weapon Diagrams, 1995. Retrieved from, https://nuclearweaponarchive.org/Library/Brown/index.html.

[16] G.H. Park, Y.Y. Cho, S.W. Kim, S.G. Hong, Analysis and DB Construction of Radioactive Xenon Isotope Characteristics for Various Types of Nuclear Threat in Neighboring Countries, 2022. NSTAR-21PS52-371.

[17] S.M. Bourret, E.M. Kwicklis, P.H. Stauffer, Evaluation of several relevant fractionation processes as possible explanation for radioxenon isotopic activity ratios in samples taken near underground nuclear explosions in shafts and tunnels, J. Environ. Radioact. 237 (2021), 106698.

[18] S.K. Lee, Y.Y. Cho, S.W. Kim, C.H. Shin, S.G. Hong, Classification of Nuclear Threat Types Using Machine Learning Techniques Based on Xenon Isotopic Activity Ratios, 2022. NSTAR-22PS52-364.